Carbohydrate Polymers 178 (2017) 260–269

Contents lists available at ScienceDirect

Carbohydrate Polymers

journal homepage: www.elsevier.com/locate/carbpol

Research Paper

Eco-friendly films prepared from plantain flour/PCL blends under reactive extrusion conditions using zirconium octanoate as a catalyst

Tomy J. Gutiérrez*, Vera A. Alvarez

Grupo de Materiales Compuestos Termoplásticos (CoMP), Instituto de Investigaciones en Ciencia y Tecnología de Materiales (INTEMA), Facultad de Ingeniería, Universidad Nacional de Mar del Plata (UNMdP) y Consejo Nacional de Investigaciones Científicas y Técnicas (CONICET), Colón 10850, B7608FLC Mar del Plata, Argentina

ARTICLE INFO

Keywords:
Active films
Antimicrobial properties
Cross-linking
Poly(ε-caprolactone)
Starch

ABSTRACT

Plantain flour (*Musa ssp.*, group AAB, sub-group clone Harton)/poly(ε-caprolactone) (PCL) blends, containing glycerol as a plasticizer, were prepared by reactive extrusion (REx) in a twin-screw extruder using zirconium octanoate ($Zr(Oct)_4$) as a catalyst, followed by thermo-compression molding for film development. The films were then characterized in terms of their: infrared (FTIR) spectra, water solubility, thermogravimetric (TGA) curves, differential scanning calorimetry (DSC) thermograms, and X-ray diffraction (XDR) diffractograms, as well as their microstructural, mechanical and antimicrobial properties in order to (1) compare the effects of PCLs with two different molecular weights (M_w) on the characteristics of the plantain flour/PCL blends, and (2) determine whether using $Zr(Oct)_4$ in the production of active composite polymer materials improves their properties. The plantain flour/PCL blends were all developed successfully. The higher M_w PCL gave more hydrophobic and thermally stable films with improved mechanical properties. The addition of the $Zr(Oct)_4$ catalyst to the plantain flour/PCL blends also resulted in films with similar characteristics to those described above, due to the cross-linking of the polymers. In addition, the films containing the catalyst showed antimicrobial activity against *Escherichia coli O157:H7* and *Staphylococcus aureus* indicating a dual effect of $Zr(Oct)_4$, and making it an attractive alternative for the development of active films.

1. Introduction

Starch-based films have been proposed as an environmentally friendly alternative to traditional food packaging materials (Gutiérrez, Guzmán, Medina Jaramillo, & Famá, 2016). This is because they are biodegradable and thus reduce, in part, the problems caused by synthetic plastics obtained from the oil industry. Recent studies have reported excellent properties of edible films made from plantain flour (Gutiérrez, Suniaga, Monsalve, & García, 2016; Pelissari, Andrade-Mahecha, Sobral, & Menegalli, 2013). Nevertheless, these materials have some drawbacks in particular their hydrophilic nature that makes them highly sensitive to water. For this reason in recent years several alternatives have been proposed to improve their properties. Among the most promising of these is the development of starch-based films blended with biopolyesters in the polyhydroxyalkanoate family (PHAs) (Gutiérrez & Alvarez, 2017a; Yu, Dean, & Li, 2006).

Poly(ε-caprolactone) (PCL) is a hydrophobic aliphatic polyester that may be obtained by chemical synthesis either from crude oil or renewable resources such as polysaccharides. PCL is a thermoplastic, biodegradable, biocompatible and semi-crystalline polymer with a very low viscosity, glass transition temperature (approx. −60 °C) and melting point (58–60 °C). In addition, PCL is a fully biodegradable and easily processable synthetic material that can be used with conventional melt processing equipment. In fact, this material is already used in the food packaging and biomedical fields (Gutiérrez & Alvarez, 2017a).

Among the advantages of using PCL are that: (1) it is a hydrophobic material with respect to other biopolymers such as proteins and therefore is not prone to plasticization or swelling, (2) it shows excellent stretchability and low water vapor permeability and (3) PCL-based films show good water resistance (Gutiérrez & Alvarez, 2017a).

Nevertheless, biopolyesters and polysaccharides are thermodynamically immiscible, *i.e.* they show a lack of polymeric compatibility owing to their different polarities. Starch-PCL blends obtained by simple mixing are thus not adequate for film preparation as their low affinity leads to phase separation. This inhibits the adhesion of the polymeric interfaces to each other resulting in poor film properties (Gutiérrez & Alvarez, 2017a). For example, Gutiérrez & Alvarez (2017a) observed phase separation in sagu flour (*Canna edulis* Kerr)/PCL and sagu starch/PCL blends, with the former showing the greater

* Corresponding author at: Institute of Research in Materials Science and Technology, Faculty of Engineering, National University of Mar del Plata and National Research Council (CONICET), P.O. Box B7608FLC, Colón 10850, Mar del Plata, Argentina.
E-mail addresses: tomy.gutierrez@fi.mdp.edu.ar, tomy_gutierrez@yahoo.es (T.J. Gutiérrez).

http://dx.doi.org/10.1016/j.carbpol.2017.09.026
Received 10 June 2017; Received in revised form 7 September 2017; Accepted 8 September 2017
Available online 18 September 2017
0144-8617/

separation. However, the use of starch-rich flours as raw materials for edible and/or biodegradable film development has generated great interest, since their high performance and low cost compared to pure starch makes them a promising alternative for the production of polymer matrices that could replace synthetic polymers obtained from oil.

Some of the disadvantages of starch/PCL blends could be solved by preparing them using reactive extrusion (REx). REx combines mass and heat transport operations which, together with simultaneous chemical reactions taking place inside the extruder, modify the properties of the existing polymers or generate new ones. The extruder can thus be considered as a reactor, where polymers can be modified in a single step while they are being processed. This procedure is increasingly becoming recognized as a powerful technique to develop and manufacture a wide variety of novel polymeric materials in a highly efficient and flexible way. The combination of chemical reactions and transport phenomena in an extruder provides an invaluable window of opportunity for the compatibilization of synthetic resins and biopolymers such as starch, or the compatibilization of synthetic resins and natural fillers under current industrial conditions (Gutiérrez & Alvarez, 2017b; Gutiérrez, Guarás, & Alvarez, 2017).

With this in mind, several catalysts have been used in conjunction with REx to generate cross-linking reactions within polymer blends especially those incorporating thermoplastic starch (TPS) (Gutiérrez & Alvarez, 2017b). The use of catalysts with REx is based on the fact that the temperatures and pressures used to process starch-based biodegradable composites activate the catalyst, thereby generating an increase in the reaction rate, *i.e.* the kinetics of the cross-linking reaction are favored. In this way, the compatibility of starch-based polymer blends can be improved by a process that is scalable industrially.

In particular, the use of octanoates as catalysts for food packaging production has generated great interest especially since some octanoates, for example tin octanoate ($Sn(Oct)_2$), are already widely used (Kowalski, Duda, & Penczek, 1998) and have been approved as food additives by the U.S. Food and Drug Administration (FDA, 2016). According to Raquez, Narayan, and Dubois (2008) the most probable reaction mechanism involves the direct catalytic action of $Sn(Oct)_2$, whereby the catalyst first activates the monomer forming a donor-acceptor complex, which then participates directly in the first propagation step. $Sn(Oct)_2$ is thereafter liberated in every ensuing propagation step. This means that Sn^{2+} atoms are not covalently bound to the polymer at any stage during polymerization. Another likely mechanism, the "active chain-end" mechanism, was proposed by Penczek et al. (2000). This involves the *in-situ* formation of Sn-alkoxide bonds at chain-ends as observed by MALDI-TOF and fully confirmed by kinetic studies (Kowalski et al., 1998). Thus, through a rapid exchange equilibrium $Sn(Oct)_2$, and most probably any other covalent metal carboxylate, is first converted by reacting with protic compounds (ROH) into tin (or other metal) alkoxides which then act as active centers for polymerization. Polymerization itself involves a "coordination insertion" mechanism similar to those reported for covalent metal alkoxides and dialkylaluminum alkoxides.

Recently our research group has used zinc octanoate ($Zn(Oct)_2$) as a catalyst in corn starch/polystyrene (PS) blends under REx conditions, observing an improvement in the compatibility between the bio- and synthetic polymers with the use of the catalyst. In addition, the $Zn(Oct)_2$ showed antimicrobial activity. Unfortunately, however, this had no effect on the developed materials possibly because its migration to the environment was compromised by the cross-linked starch/PS network (Gutiérrez & Alvarez, 2017b). With all this in mind we feel that it is worth examining the potential dual function (catalyst and antimicrobial agent) of another octanoate, zirconium octanoate ($Zr(Oct)_4$), for the production of active eco-friendly materials for food packaging. It is worth noting that there is currently no record in the literature of the use of $Zr(Oct)_4$ in food packaging systems.

In addition, most of the studies found in the literature related to starch materials have focused on films obtained by the casting method, whereas processing methods such as blown film extrusion, compression, or injection molding are less reported. Solvent casting is the most common method employed for small-scale biopolymer film preparation and involves solubilization, casting, and drying steps. Despite this being a good and adequate technique on a laboratory scale, it is considered to be a high energy-consuming procedure and thus not appropriate for large-scale production (Gutiérrez & Alvarez, 2017c).

Procedures for the efficient manufacture of high quality, biodegradable films are thus still required by industry. With this in mind, the scaling-up of processing methods using equipment designed for synthetic polymers is indispensable, and extrusion, blowing, injection and thermo-compression are all viable alternatives due to their energy efficiency and high productivity. In particular, extrusion followed by thermo-compression is useful as a processing method because of its simplicity. These techniques could thus be used to provide feasible ways of developing biomaterials that are both economical and environmentally friendly (Gutiérrez & Alvarez, 2017c).

The aims of this study were thus to (1) compare the effects of using low and high molecular weight (M_w) PCL on the properties of plantain flour/PCL blends and (2) determine whether the use of $Zr(Oct)_4$ can improve the properties of active composite polymer materials.

2. Experimental

2.1. Materials

Plantain flour (*Musa ssp.,* group AAB, sub-group clone Harton) was obtained by the method described by Pacheco (2001). The plantains were purchased at a local market in Caracas, Venezuela, and had a degree of maturation of 1 according to the scale put forward by Loesecke (1950), *i.e.* unripe fruit. The plantain flour obtained was characterized in terms of its moisture content (9.4%), total proteins (2.64%), crude fat (0.36%), ash (2.41%), crude fiber (0.297%), total carbohydrates (84.9%), starch content (85%), amylose content (24%) and average molecular weight (M_w) (70×10^6 g/mol) (Gutiérrez & Álvarez, 2016). Poly(ε-caprolactone) (PCL) pellets with molar weights (M_w) of 10,000 and 80,000 g/mol were purchased from Aldrich (product codes: 440744-500G and 440752-500G, respectively) and used to prepare the plantain flour/PCL blends. The catalyst (zirconium 2-ethylhexanoate [IUPAC name] – zirconium octanoate [trade name] – $Zr(C_8H_{15}O_2)_4$ [molecular formula] – $Zr(Oct)_4$ [condensed molecular formula]; density = 0.870 g/mL at 25 °C; and boiling point = 167–178 °C at 760 mmHg) was kindly provided by Ghion, Laboratorios Químicos, S.R.L. (Mar del Plata, Argentina) (approx. 12% w/w of Zr). Glycerol (density = 1.26 g/mL; boiling point = 290 °C) (Aurum, Mar del Plata, Argentina) was employed as the plasticizer for film formation.

2.2. Extrusion and film formation

Films were prepared from plantain flour, and plantain flour/PCL blends at a 50:50 ratio (152.5 g of starch and 152.5 g of PCL), plus 67.5 g of glycerol. To some of the samples 10 mL of the catalyst were then also added. The blends were homogenized manually before being introduced into the extruder. The instrument used was a twin-screw extruder with six heating zones and two feed zones. The first feed zone is in the first heating step and the second in the third heating step. The extrusion profile selected was 50/70/90/100/100/100 °C. Films were obtained by compressing at 130 °C for 15 min at 100 bar and then cooling to 30 °C. Five film systems were obtained as follows: plantain flour (*TPPF*); plantain flour + PCL (M_w = 10,000 g/mol) (*TPPF/PCL (10,000)*); plantain flour + PCL (M_w = 10,000 g/mol) + catalyst (*TPPF/PCL(10,000) + CAT*); plantain flour + PCL (M_w = 80,000 g/mol) (*TPPF/PCL(80,000)*); and plantain flour + PCL (M_w = 80,000 g/

mol) + catalyst (*TPPF/PCL(80,000) + CAT*). The resulting materials were conditioned with a saturated NaBr solution (a_w ~0.575 at 25 °C) for seven days prior to each test.

2.3. Characterization of the films

2.3.1. Attenuated total reflectance fourier transform infrared spectroscopy (ATR/FTIR)

The IR spectra of the films were determined using a Nicolet 8700 infrared spectrometer (FTIR) (Thermo Scientific Instrument Corporation, Madison, Wisconsin, USA) equipped with a diamond at an incident angle of 45° to collect the infrared spectra of the film samples. The spectra were recorded in Attenuated Total Reflectance mode (ATR) between 700 and 4000 cm^{-1}, using 40 scans at a resolution of 4 cm^{-1}. Each sample was scanned three times observing good reproducibility.

2.3.2. Water solubility (WS)

Water solubility (WS) was determined according to the method described by Gutiérrez, Morales, Pérez, Tapia, and Famá (2015). Film pieces were cut (2 × 2 cm) and the initial weights registered (w_i). The initial dry matter content of each film system was determined by drying them to a constant weight in an oven (Memmert, Germany) at 105 °C. To determine the weight of dry matter not solubilized in water the film pieces were immersed in 50 mL of distilled water and stored for 24 h at 25 °C. After this, they were filtered through previously desiccated and weighed filter paper, and the undissolved films obtained dried again to a constant weight (w_f) in the same oven at 105 °C for 24 h. The solubility of each film system was then determined as follows:

$$WS(\%) = (w_i - w_f) \times w_i^{-1} \times 100 \quad (1)$$

where w_i and w_f are the initial and final weights of each sample, respectively. Results were reported as % water solubility ± standard deviation (SD) from three measurements per film system.

2.3.3. Thermogravimetric analysis (TGA)

Thermogravimetric tests were carried out with a thermal analyzer (Model TGA Q500, Hüllhorst, Germany). Samples were heated at a constant rate of 10 °C/min from room temperature up to 500 °C under a nitrogen flow of 30 mL/min. Film weights were in the range of 13–17 mg. Analyses were performed in triplicate to ensure repeatability.

2.3.4. Differential scanning calorimetry (DSC)

A DSC-50 differential thermal analyzer (Shimadzu Corporation, Oregon, USA) was used to determine the melting temperatures (T_m) of the different films. The temperature and heat flux of the instrument were previously calibrated using indium and zinc. About 5 mg of each sample was placed in hermetically sealed aluminum pans and heated from room temperature up to 110 °C at a scanning rate of 10 °C/min. under a nitrogen atmosphere. Changes of phase or state and the corresponding enthalpies were determined from the melting peaks of the DSC thermograms (Biliaderis, Lazaridou, & Arvanitoyannis, 1999). The crystallinity percentage values of each sample were then calculated according to the following equation (Merino, Ludueña, & Alvarez, 2017):

$$\text{Crystallinity}(\%) = \left({}^{\Delta H_m}\!/_{w_{PCL} x \Delta H_{100}} \right) \times 100 \quad (2)$$

where ΔH_m is the experimental melting enthalpy, w_{PCL} is the PCL weight fraction and ΔH_{100} is the melting enthalpy of 100% crystalline PCL (142 J/g) (Tsuji & Ishizaka, 2001). Three samples were analyzed for each film system. The crystallinity percentage values ± SD were reported from three samples for each film system.

2.3.5. X-ray diffraction (XRD)

X-ray diffractograms of the different films were obtained with a PAN analytical X'Pert PRO diffractometer (Netherlands) equipped with a monochromatic Cu K_α radiation source (λ = 1.5406 Å) operating at a voltage of 40 kV and current 40 mA at a scanning rate of 1° per min. The scanning region of the samples was in a 2θ range between 3° and 33°. The distances between the planes of the crystals d (Å) were calculated from the diffraction angles (°) measured from the X-ray diffractograms according to Bragg's law:

$$n\lambda = 2d\sin(\theta) \quad (3)$$

where λ is the Cu K_α radiation wavelength and n is the order of reflection. For the calculations, n was taken as 1. The thicknesses of the samples on the slides were ~1.12 mm. The crystallinity percentage values of each film were also calculated taking into account the main peaks (main d-spacings) as described by Hermans & Weidinger (1961) by the following equation:

$$\text{Crystallinity}(\%) = \left({}^{A_c}\!/_{A_c + A_a} \right) \times 100 \quad (4)$$

where A_c is the crystalline area, A_a is the amorphous area, and $A_c + A_a$ is the total area under each of the curves of the different X-ray diffractograms. Percentage crystallinity was determined to verify the results obtained by the DSC calculations.

2.3.6. Scanning electron microscopy (SEM)

Both the surfaces and the cryo-fractured surfaces of the thermocompressed films were analyzed using a JEOL JSM-6460 LV scanning electron microscope. Films were cryo-fractured by immersion in liquid nitrogen. For both analyses the films were mounted on bronze stubs and sputter-coated (Sputter coater SPI Module, Santa Clara, CA, USA) with a thin layer of gold for 35 s.

2.3.7. Uniaxial tensile tests

The mechanical properties of the films were determined from samples cut in a bone-shape with an effective area of ~28.6 mm long × ~5.5 mm width and cross-sectional area ~6.5 mm^2 (the exact value differed slightly between samples). Film samples (10 per formulation) were mounted and clamped with tensile grips (A/TG model) in an INSTRON 4467 machine to generate the force-distance curves following the ISO 527-2 (2012) norm. The samples were stretched at a constant speed of 0.01 mm/s at 25 °C until they broke.

The overall stress acting on each sample during tension was expressed as the so-called true tensile strength (σ). This is the force normal to the film cross-section $F(N)$ divided by the initial area A_0 (m^2) of the sample (Hamann, Zhang, Daubert, Foegeding, & Diehl, 2006):

$$\sigma = {}^{F}\!/_{A_o} \quad (5)$$

The overall strain (ε) of each film was expressed as a percentage of the initial height as follows:

$$\varepsilon = {}^{L}\!/_{L_o} \times 100\% \quad (6)$$

where Lo and L (mm) are the initial and final longitudes of each film before and after deformation, respectively.

The mechanical properties at break: maximum stress (σ_m) and strain at break (ε_b) were obtained from the stress-distance curves. For this, the curves were transformed into stress-strain curves as outlined in ISO 527-2 (2012). Young's modulus (E) was then determined from the linear regression slope of the stress-strain curves, and toughness (T) was calculated from the area under the stress-strain curves.

2.3.8. Antimicrobial activity

Antimicrobial activity tests of the films were carried out using the agar diffusion method according to Gutiérrez & Alvarez (2017b). Films were cut into circular-shaped discs (diameter 12 mm) and hydrated with 1 mL of sterile water. They were then placed on Mueller Hinton agar plates (Merck, Darmstadt, Germany) previously seeded with

0.1 mL of inoculum containing approximately 10^5–10^6 CFU/mL each of the two pathogenic bacteria (one Gram-negative and the other Gram-positive) tested: *Escherichia coli O157:H7* (32158, American Type Culture Collection) and *Staphylococcus aureus*, respectively, both of which were provided by the Centro de Referencia de Lactobacilos (CERELA, Tucumán, Argentina). The zone of inhibition assay on solid media was used for determining the antimicrobial effect of each film. Plates were incubated for 24 h at 37 °C and then examined to study the inhibitory effect. The total area was used to evaluate the antimicrobial potential of the films by exactly measuring the diameter of the inhibitory zones surrounding the wells as well as the contact area of these with the agar surface. The films were then evaluated according to Ponce, Fritz, del Valle, and Roura (2003) who classified the susceptibility of microorganisms to a given inhibitory agent based on the diameters of inhibition halos as: not sensitive, sensitive, very sensitive and extremely sensitive. Experiments were done in triplicate on two separate experimental runs.

2.4. Statistical analysis

The experimental data was analyzed using OriginPro 8 (Version 8.5, Northampton, USA) software. The results were expressed as means ± SD, and the one-way ANOVA procedure followed by Duncan's multiple range tests was adopted to determine significant differences ($p < 0.05$) between treatments.

3. Results and discussion

3.1. Attenuated total reflectance fourier transform infrared spectroscopy (ATR/FTIR)

Fig. 1A shows the ATR/FTIR spectra of the different films studied over the whole absorption range. A significant absorption peak at around 3309 cm^{-1} associated with the stretching of the OH groups belonging to the starch, glycerol and water and the stretching vibration of the C—O groups was observed in all the systems studied (Pereira, de Arruda, & Stefani, 2015). Gutiérrez (2017) suggested that materials with more free OH groups vibrate more easily and thus tend to present wider bands with higher absorbance. It can thus be inferred from Fig. 1B that the number of OH groups in each of the film formulations decreased in the following order: TPPF > TPPF/PCL (10,000) > TPPF/PCL(10,000) + CAT > TPPF/PCL (80,000) > TPPF/PCL(80,000) + CAT. Shi et al. (2007) proposed another method to compare the number of available OH groups in these types of systems: the ratio between the band intensities at 3300 cm^{-1} (I_{3300}) and 1149 cm^{-1} (I_{1149}) (A_{3300}/A_{1149} ratio). This was 1.03, 0.54, 0.50, 0.32 and 0.27 for the TPPF, TPPF/PCL(10,000), TPPF/PCL (10,000) + CAT, TPPF/PCL(80,000) and TPPF/PCL(80,000) + CAT films, respectively. Both methods thus gave the same results. As expected, the films containing poly(ε-caprolactone) (PCL) had fewer OH groups than those without PCL. The fewer the number of OH groups the more hydrophobic the material, thus showing that the incorporation of this hydrophobic polymer reduced the hydrophilicity of the flour/PCL blends. The films with the high molecular weight (M_w) PCL contained the fewest free OH groups, particularly those with the added catalyst (zirconium octanoate – $Zr(Oct)_4$). In the latter case this was possibly due to the cross-linking of the starchy matrix and the PCL. Similar results have been reported by Gutiérrez & Alvarez (2017b) for films developed from corn starch/polystyrene (PS) blends using zinc octanoate ($Zn(Oct)_2$) under reactive extrusion (REx) conditions.

The band located at 1716 cm^{-1} (Fig. 1A) in the PCL-containing films represents the C=O groups of the esters in the PCL, thus confirming their presence. An increase in the intensity of this band can be seen in Fig. 1C for the films containing the catalyst (TPPF/PCL(10,000) + CAT and TPPF/PCL(80,000) + CAT) compared to the analogous films prepared without the catalyst (TPPF/PCL(10,000) and TPPF/PCL (80,000)). This could be related to the formation of new C=O groups in the esters formed between the plantain flour and the PCL during cross-linking. Interestingly, there is a more significant increase in the intensity of the band located at 1716 cm^{-1} in the TPPF/PCL(80,000) + CAT films than the TPPF/PCL(10,000) + CAT films, thus suggesting a higher degree of cross-linking between the plantain flour and the higher M_w PCL in the presence of the catalyst.

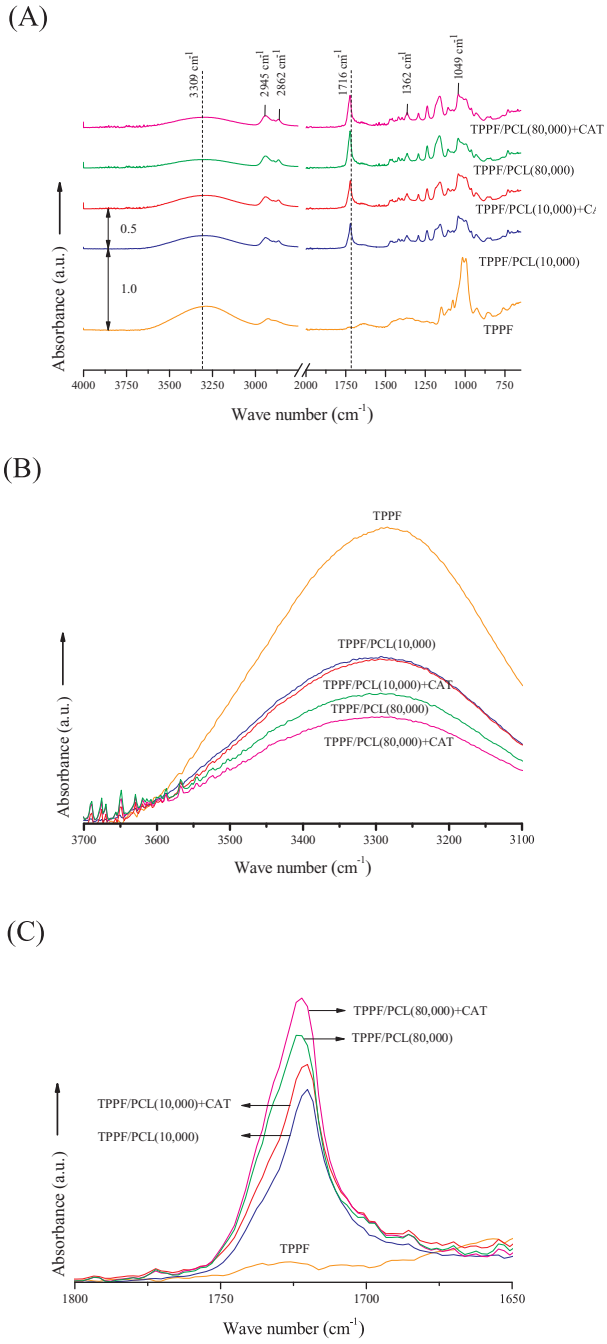

Fig. 1. Panel A- FTIR spectra of the different films studied in all the absorption range. **Panel B**- FTIR spectra in the absorption range corresponding to C—O group (OH stretching) of the different films studied. **Panel C**- FTIR spectra in the absorption range corresponding to C=O group. Film systems: plantain flour (TPPF), plantain flour + PCL (M_w = 10,000 g/mol) (TPPF/PCL(10,000)), plantain flour + PCL (M_w = 10,000 g/mol) + catalyst (TPPF/PCL(10,000) + CAT), plantain flour + PCL (M_w = 80,000 g/mol) (TPPF/PCL(80,000)) and plantain flour + PCL (M_w = 80,000 g/mol) + catalyst (TPPF/PCL(80,000) + CAT).

Other peaks located at 2862 and 2945 cm^{-1} are associated with C—H stretch vibrations (Mathew, Brahmakumar, & Abraham, 2006) and

Table 1
Water solubility (*WS*) and crystallinity percentages of the films studied.

Parameter	TPPF	TPPF/PCL(10,000)	TPPF/PCL(10,000) + CAT	TPPF/PCL(80,000)	TPPF/PCL(80,000) + CAT
WS (%)	30.8 ± 0.5^{c}	26.3 ± 0.3^{b}	27.1 ± 0.5^{b}	25.1 ± 0.4^{a}	25.6 ± 0.3^{a}
Crystallinity (%)	< 1^{a}	36 ± 1^{b}	49 ± 1^{c}	35 ± 1^{b}	62 ± 1^{d}

Equal letters in the same row indicate no statistically significant differences ($p \leq 0.05$).
Film systems: plantain flour (TPPF), plantain flour + PCL (M_w = 10,000 g/mol) (TPPF/PCL(10,000)), plantain flour + PCL (M_w = 10,000 g/mol) + catalyst (TPPF/PCL(10,000) + CAT), plantain flour + PCL (M_w = 80,000 g/mol) (TPPF/PCL(80,000)) and plantain flour + PCL (M_w = 80,000 g/mol) + catalyst (TPPF/PCL(80,000) + CAT).

are characteristic of polymeric matrix materials, and the bands observed between 1362 cm^{-1} and 1497 cm^{-1} are assigned to C—O angular deformations (Batista Reis et al., 2015). Specifically, the band detected at ~1049 cm^{-1} in all the films developed is associated with —C—O—C— glycosidic bonds (Gutiérrez, 2017).

3.2. Water solubility (WS)

Table 1 shows the water solubility values at 25 °C for the different films studied. As can be observed all of the films made from the plantain flour/PCL blends, with and without the catalyst, were significantly less water soluble ($p \leq 0.05$) than the films prepared from plantain flour alone (TPPF). These results were expected as the hydrophilic nature of a starchy matrix should decrease when blended with a hydrophobic polymer such as PCL. In addition, the incorporation of the high M_w PCL in the plantain flour/PCL blends resulted in a significant decrease in the water solubility ($p \leq 0.05$) of the TPPF/PCL(80,000) and TPPF/PCL (80,000) + CAT films compared to the films made with the low M_w PCL blends (TPPF/PCL(10,000) and TPPF/PCL(10,000) + CAT). According to the results obtained from the FTIR spectra, this is associated with the lower number of OH groups available in these blends. The water solubility of starch films thus provides an indication of their integrity in an aqueous medium, such that higher solubility values indicate a lower water resistance (Romero-Bastida et al., 2005). To summarize: blends made with the high M_w PCL gave films with improved water resistance. These results agree with the FTIR spectra analyses.

Likewise, the results obtained from the FTIR spectra suggest that the incorporation of the catalyst into the polymer blends (TPPF/PCL (10,000) + CAT and TPPF/PCL(80,000) + CAT) leads to a decrease in the number of free OH groups. However, the water solubility of the films with and without the catalyst, (TPPF/PCL(10,000) + CAT and TPPF/PCL(80,000) + CAT) *vs* (TPPF/PCL(10,000) and TPPF/PCL (80,000), respectively) were not statistically different ($p \geq 0.05$). We cannot thus confirm yet that the presence of the catalyst caused a reduction in the number of free OH groups in the films studied. Nevertheless, other studies have reported that the addition of a catalyst under REx conditions does decrease the water solubility of films made from starch/synthetic polymer blends (Gutiérrez & Alvarez, 2017b).

3.3. Thermogravimetric analysis (TGA)

The TGA curves for the systems under study are given in Fig. 2. This assay was conducted in order to analyze the thermal stability of the five types of film prepared. According to Pelissari et al. (2013) and Gutiérrez & Álvarez (2016) the thermal decomposition of glycerol-starch-containing films occurs in three main stages. The first stage of degradation, at around 100 °C, sees the onset of weight loss associated with moisture loss. During the second stage, between 160 and 290 °C, the glycerol-rich phase, which also contains starch, evaporates. Finally, in the third stage at temperatures above 330 °C, the degradation of the partially decomposed starch is completed (Sanyang, Sapuan, Jawaid, Ishak, & Sahari, 2015).

The first fact worth noting from the TGA curves is the double weight loss shown by the TPPF film. This is related to an obvious phase separation caused by the low compatibility of the flour-glycerol blend.

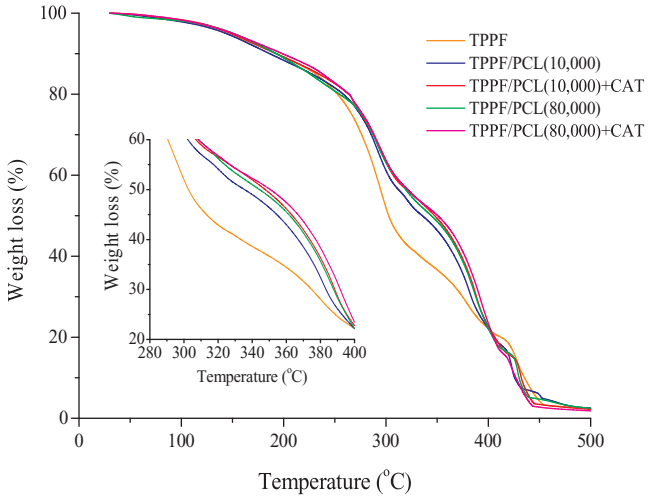

Fig. 2. TGA curves of the films studied: plantain flour (TPPF), plantain flour + PCL (M_w = 10,000 g/mol) (TPPF/PCL(10,000)), plantain flour + PCL (M_w = 10,000 g/mol) + catalyst (TPPF/PCL(10,000) + CAT), plantain flour + PCL (M_w = 80,000 g/mol) (TPPF/PCL(80,000)) and plantain flour + PCL (M_w = 80,000 g/mol) + catalyst (TPPF/PCL(80,000) + CAT).

Similar results have been reported by Gutiérrez, Suniaga et al. (2016) and Gutiérrez and Álvarez (2016) for films also prepared from plantain flour, but obtained by casting. The phase separation observed in the TPPF film suggests that the plasticizer (glycerol) is free, and is thus more easily solubilized in water resulting in a more soluble system. This agrees with the results obtained from the FTIR spectra: the TPPF film had the highest A_{3300}/A_{1149} ratio indicating a higher number of available OH groups.

On the other hand, only a low degree of phase separation was observed for the films made from the plantain flour/PCL blends, which was far less obvious than that of the TPPF films. These results were not expected as it is widely known that the polymers used, *i.e.* starch/PCL, are immiscible. Nonetheless, it came as a welcome surprise and may be because the lipids contained in the chemical composition of the plantain flour acted as compatibilizing agents between the starch contained in the flour and the PCL. This would also explain the decrease in the water solubility observed for the flour/PCL film systems.

Another important result to highlight is that the films made with the high M_w PCL (TPPF/PCL(80,000) and TPPF/PCL(80,000) + CAT blends) showed higher degradation temperatures than those made with the low M_w PCL blends (TPPF/PCL(10,000) and TPPF/PCL(10,000) + CAT) (Fig. 2). It is well known that polymer systems with higher M_w tend to have higher thermal resistance. This is in line with the results obtained. In addition, using a high M_w PCL in the presence of a catalyst under REx conditions increases the degree of the cross-linking reactions, demonstrated by a further increase in the thermal degradation temperature of these carbohydrate-based polymers. The results discussed so far thus provide evidence of the cross-linking of the polymeric matrices in the catalyst ($Zr(Oct)_4$)-containing films (TPPF/PCL(10,000) + CAT and TPPF/PCL(80,000) + CAT) processed under REx conditions. Similar results were reported by Gutiérrez & Álvarez (2016) for plantain flour based films using *aloe vera* gel as a cross-linking agent.

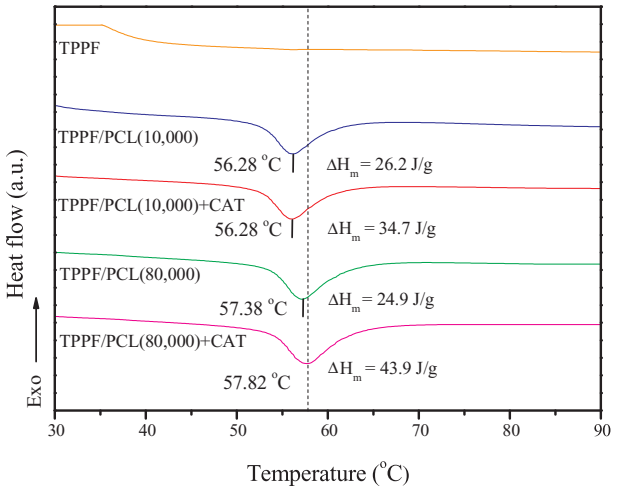

Fig. 3. Heating thermograms of the films studied: plantain flour (TPPF), plantain flour + PCL (M_w = 10,000 g/mol) (TPPF/PCL(10,000)), plantain flour + PCL (M_w = 10,000 g/mol) + catalyst (TPPF/PCL(10,000) + CAT), plantain flour + PCL (M_w = 80,000 g/mol) (TPPF/PCL(80,000)) and plantain flour + PCL (M_w = 80,000 g/mol) + catalyst (TPPF/PCL(80,000) + CAT).

A positive effect of the use of the catalyst under REx conditions to produce the flour/PLC blends was a slight tendency to avoid phase separation, possibly related to the cross-linking between the polymers used.

3.4. Differential scanning calorimetry (DSC)

Fig. 3 shows the DSC curves for the developed films. According to Labet & Thielemans (2009) the melting temperature (T_m) of PCL is between 56 and 65 °C. The endothermic peaks of the film systems prepared from plantain flour/PCL blends were thus consistent with the T_m of the crystalline fraction of the PCL.

As a general rule any structural feature that reduces the mobility of the polymer chains or the free volume will increase the T_m (Mitrus, 2005). The increase in the T_m of the systems containing the high M_w PCL (TPPF/PCL(80,000) and TPPF/PCL(80,000) + CAT) can thus be attributed to the lower mobility and rearrangement of the macromolecules of this PCL. Gutiérrez & Alvarez (2017b) concluded that the increase they found in the T_m of film systems made from starch/PS was associated with cross-linking between the polymeric matrices when Zn $(Oct)_2$ was used as the catalyst under REx conditions. The slight increase in the T_m of the TPPF/PCL(80,000) + CAT films compared to the TPPF/PCL(80,000) films can thus be attributed to the cross-linking between the plantain flour and the PCL, triggered by the use of the catalyst. Thus the reduction in the number of available OH groups in these systems (see Section 3.1) was brought about by the cross-linking reactions of starch chains that occur through these hydroxyl groups, which act as nucleophiles in the addition reaction on the double bond of the caprolactone monomer (Gutiérrez & Alvarez, 2017b). Nevertheless, no significant differences were observed in the T_m of the TPPF/PCL (10,000) + CAT films compared to the TPPF/PCL(10,000) films.

In addition, higher melting enthalpy values (ΔH_m) values have been correlated with the strengthening of inter and intramolecular interactions between starch-starch chains and starch-synthetic polymer chains (Gutiérrez, 2017; Gutiérrez & Alvarez, 2017b; Mali et al., 2002). According to Bertuzzi, Castro Vidaurre, Armada, & Gottifredi (2007) the cross-linking reactions between the polymers cause the starch molecules to align leading to an increase in the growth rate of the crystalline phase in these semi-crystalline biomaterials. Thus the higher ΔH_m values of the catalyst-containing films (TPPF/PCL(10,000) + CAT and TPPF/PCL(80,000) + CAT) compared to those of the films prepared without the catalyst (TPPF/PCL(10,000) and TPPF/PCL(80,000)) confirm that cross-linking has occurred between the plantain flour and the PCL. This agrees with the rest of the results discussed above.

The crystallinity percentages of all the systems were calculated from the ΔH_m values following the methodology proposed by Merino et al. (2017) (Table 1). The TPPF films were almost completely amorphous (< 1% crystallinity), whilst the films made from flour plantain/PCL blends were significantly more crystalline ($p \leq 0.05$). Obviously these results are due to the semi-crystalline nature of PCL as reported in the literature (Gutiérrez & Alvarez, 2017a). It is worth noting that no statistically significant differences in percent crystallinity ($p \geq 0.05$) were observed between the TPPF/PCL(10,000) and TPPF/PCL(80,000) films. However, the films containing the catalyst (TPPF/PCL(10,000) + CAT and TPPF/PCL(80,000) + CAT) were significantly more crystalline ($p \leq 0.05$) than the films prepared without it (TPPF/PCL(10,000) and TPPF/PCL(80,000)). This confirms that it was the action of the catalyst that generated the cross-linking reactions between the polymer matrices under REx conditions. As mentioned previously, the cross-linking reactions caused the polymers to align in parallel leading to a rise in the crystallinity of these systems (Gutiérrez, Tapia, Pérez, & Famá, 2015). This had a positive effect on the films, since cross-linking inhibits the retrogradation of these types of materials resulting in improved mechanical properties (García-Tejeda et al., 2013). An even more significant increase ($p \leq 0.05$) in the percent crystallinity was obtained by incorporating a higher M_w PCL in the presence of the catalyst (TPPF/PCL(80,000) + CAT film) suggesting that increasing the M_w of the PCL generated a higher rate of reactivity in the catalyst compared to the TPPF/PCL(10,000) + CAT film. This may be due to an increase in the number of active sites on the PCL leading to an increase in the reaction (cross-linking) rate. Thus it seems that the use of higher M_w PCL can result in a higher degree of cross-linking.

3.5. X-ray diffraction (XRD)

Fig. 4A shows the X-ray diffractograms and percent crystallinities of the films studied. It can be observed that the results obtained by XRD agree with those of the DSC. Thus, in general, both the methodologies used to determine percent crystallinity (Hermans & Weidinger, 1961 – XRD and Merino et al., 2017 – DSC) gave the same results. Specifically, the TPPF film shows a spectrum typical of an amorphous material, in line with the crystallinity percentage values calculated.

The films made with the PCL showed the characteristic peaks of the crystallinity of this polymer at 2θ = 21.2°, 21.8° and 23.5°, corresponding to the *d*-spacings ≅ 4.2 Å, 4.1 Å, and 3.8 Å, respectively (Ninago et al., 2015). Similar results were reported by Ortega-Toro, Contreras, Talens, & Chiralt (2015) for starch-based films with different starch-PCL ratios.

On the other hand, it is evident from Fig. 4B that the peak at 2θ = 21.2° exhibits a slight displacement towards lower 2θ values in the films containing the catalyst (TPPF/PCL(10,000) + CAT and TPPF/PCL(80,000) + CAT) indicating an increase in the molecular spacing of the polymer chains.

3.6. Scanning electron microscopy (SEM)

Fig. 5 shows the SEM images of the thermo-compressed and cryo-fractured surfaces of the different films. The thermo-compressed surfaces were very smooth and flat except for the films containing the catalyst (TPPF/PCL(10,000) + CAT and TPPF/PCL(80,000) + CAT) which had some cracks.

The cryo-fractured surfaces of the films derived from the plantain flour/PCL blends were very heterogeneous, demonstrating the immiscibility of the polymers (plantain flour and PCL). This is consistent with the TGA results. Similar structures were reported by Ortega-Toro et al. (2015) and Gutiérrez & Alvarez (2017b) for films prepared from starch/PCL blends in different proportions, and for films made from sagu starch and flour/PCL blends, respectively.

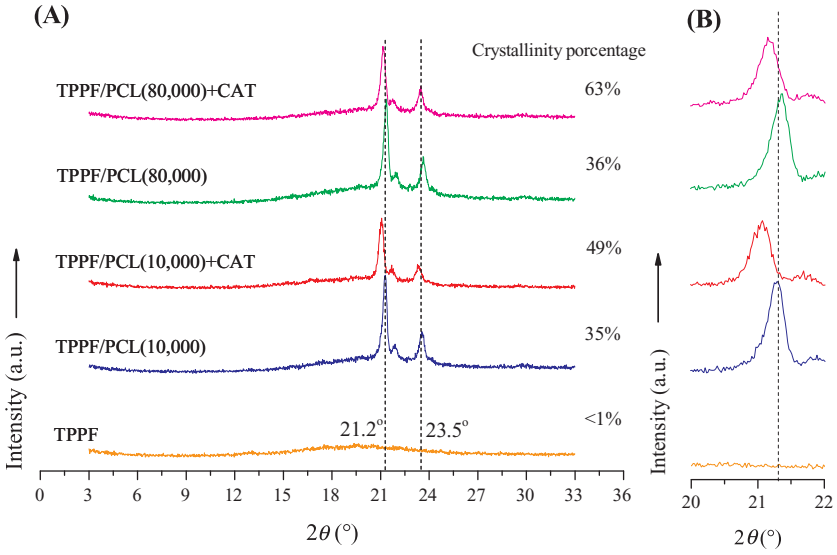

Fig. 4. Panel A- X-ray diffraction diffractograms in the range of 3 – 33° (*2θ*) and crystallinity percentages of the film systems studied. **Panel B**- X-ray diffraction diffractograms in the range of 20 – 22° (*2θ*) of the film systems. Film systems: plantain flour (TPPF), plantain flour + PCL (M_w = 10,000 g/mol) (TPPF/PCL(10,000)), plantain flour + PCL (M_w = 10,000 g/mol) + catalyst (TPPF/PCL(10,000) + CAT), plantain flour + PCL (M_w = 80,000 g/mol) (TPPF/PCL(80,000)) and plantain flour + PCL (M_w = 80,000 g/mol) + catalyst (TPPF/PCL (80,000) + CAT).

Finally, none of the surfaces of the films examined showed structures similar to starch granules. We can thus assume that the processing conditions selected produced the complete gelatinization of the starch.

3.7. Uniaxial tensile tests

The stress-strain curves of the developed films are shown in Fig. 6A. The mechanical behavior of the films made from the plantain flour and low M_w PCL blends (TPPF/PCL(10,000) and TPPF/PCL(10,000) + CAT) could not be assessed as they were too fragile (see Fig. 6B and C). The results outlined above are also consistent with the TGA results which indicated a higher thermal resistance in films made from plantain flour/high M_w PCL blends (TPPF/PCL(80,000) and TPPF/PCL (80,000) + CAT). It thus seems that the improvements observed in the mechanical properties of the high M_w PCL systems are related to the greater molecular interactions that occur within them. Cheung, Lau, Lu, and Hui (2007) reported similar results for high M_w polyethylene glycol (PEG) films.

With regard to the other films, a small linear elastic zone followed by a non-linear zone was observed until break point in the TPPF film, and in the films containing the high M_w PCL (TPPF/PCL(80,000) and TPPF/PCL(80,000) + CAT) a creep zone was observed. The presence of a creep zone indicates a change in mechanical behavior from an elastic to a plastic zone, and was irreversible from 0.59% elongation in the TPPF/PCL(80,000) film and 0.54% elongation in the TPPF/PCL (80,000) + CAT film. In other words, theoretically, after elastic deformation these materials undergo a volume change.

The TPPF/PCL(80,000) + CAT film had a smaller creep zone than the TPPF/PCL(80,000) film, a result similar to that reported by Gutiérrez & Alvarez (2017b) for films made from starch/PS blends using $Zn(Oct)_2$ as a catalyst under REx conditions. It is well known that after the creep zone, Hooke's Law for elastic, linear and isotropic materials is not met. This means that normal deformation does not occur anywhere in the solid, nor along any of the normal stresses in the orthogonal directions, *i.e.* the principal directions of the stress matrix do not coincide with the principal direction of the matrix of deformation (Gutiérrez & Alvarez, 2017b).

In addition, the positive slope of the curve in the plastic deformation range for the films containing the catalyst (TPPF/PCL(80,000) + CAT) implies that hardening occurred until the sample finally broke. This correlates with the assertion that the polymer chains in these films were aligned parallel to the load (Berruezo, Ludueña, Rodriguez, & Alvarez, 2014) and fits well with the crystallinity results obtained by both DSC and XRD for this system (TPPF/PCL(80,000) + CAT) as compared to

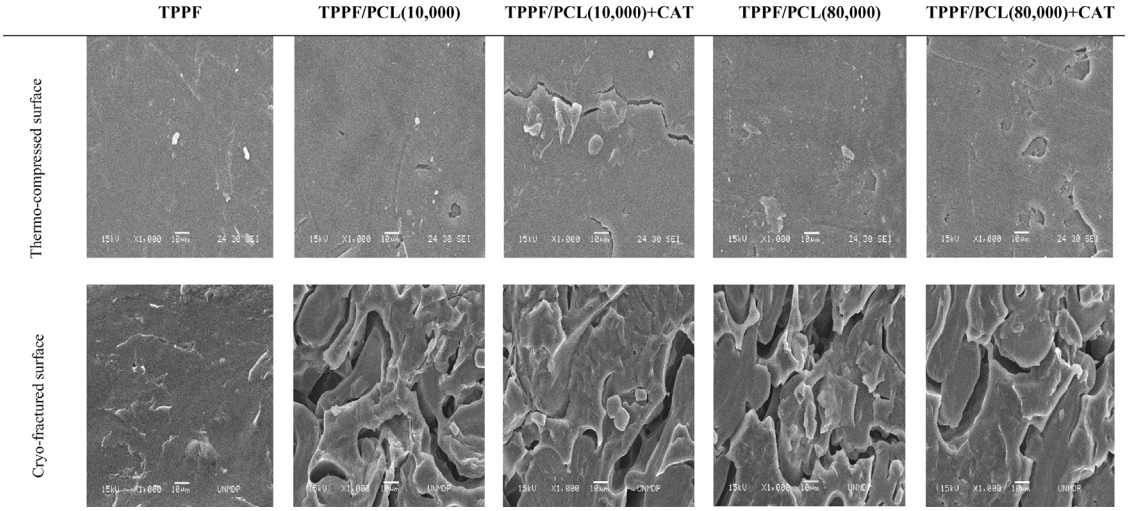

Fig. 5. SEM micrographs of the thermo-compressed and the cryo-fractured surfaces of the films studied: plantain flour (TPPF), plantain flour + PCL (M_w = 10,000 g/mol) (TPPF/PCL (10,000)), plantain flour + PCL (M_w = 10,000 g/mol) + catalyst (TPPF/PCL(10,000) + CAT), plantain flour + PCL (M_w = 80,000 g/mol) (TPPF/PCL(80,000)) and plantain flour + PCL (M_w = 80,000 g/mol) + catalyst (TPPF/PCL(80,000) + CAT). At 1 kX of magnification.

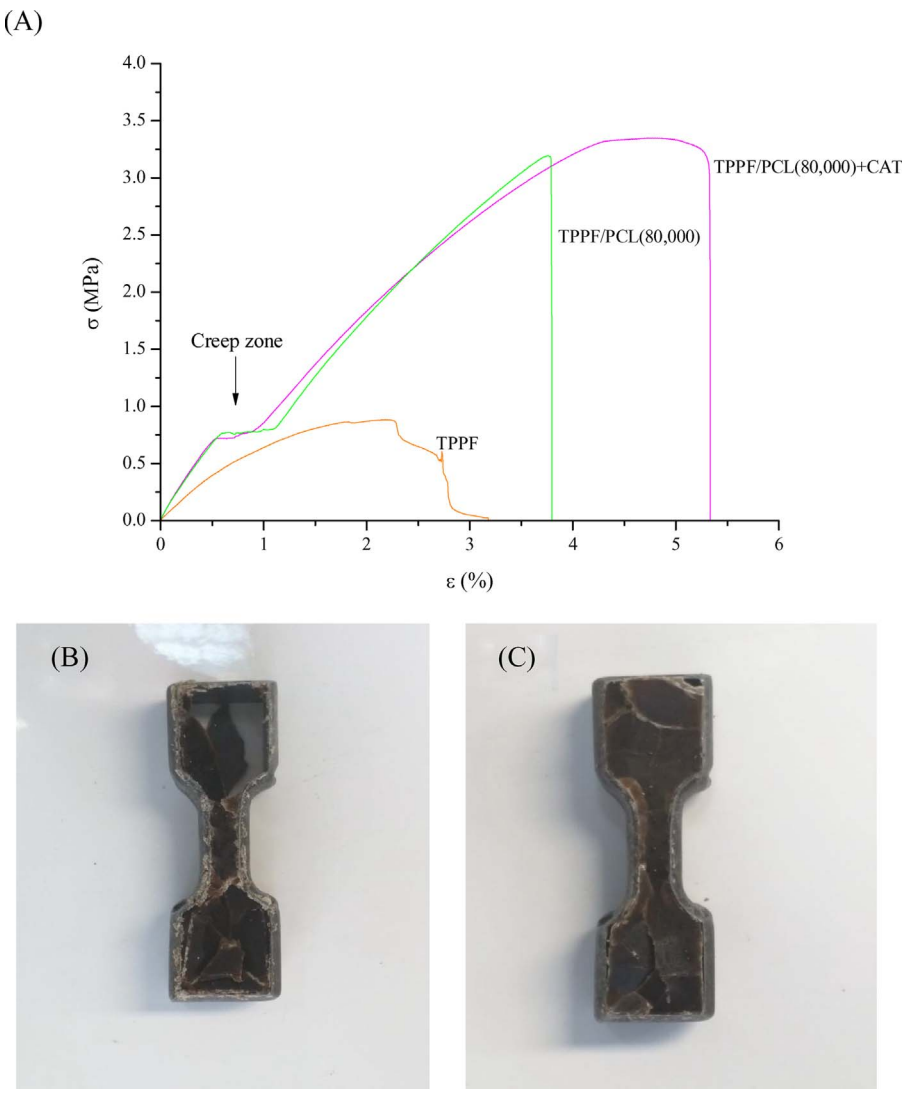

Fig. 6. Panel A- Stress (σ)-strain (ε) curves of the films studied: plantain flour (TPPF), plantain flour + PCL (M_w = 80,000 g/mol) (TPPF/PCL(80,000)) and plantain flour + PCL (M_w = 80,000 g/mol) + catalyst (TPPF/PCL (80,000) + CAT). **Panel B**- Appearance of the film prepared from plantain flour + PCL (M_w = 10,000 g/mol) (TPPF/PCL (10,000)). **Panel C**- Appearance of the film prepared from plantain flour + PCL (M_w = 10,000 g/mol) + catalyst (TPPF/PCL(10,000) + CAT).

the analogous films prepared without the use of the catalyst (TPPF/PCL (80,000)). Once again, the results obtained confirm the cross-linking of the plantain flour with the PCL under REx conditions using $Zr(Oct)_4$ as a catalyst.

It is important to note, however, that the mechanical properties observed for the TPPF/PCL(80,000) and TPPF/PCL(80,000) + CAT films would signify the failure of these materials in a kinematic system. They are thus not appropriate for food packaging applications where the duration of the stress, the applied load and temperature are important considerations.

Generally the Young's modulus and maximum stress values of films made from 50/50 flour/PCL blends significantly increase ($p \leq 0.05$) compared to films that do not contain PCL independently of whether they are processed by blending or extrusion (Table 2). The incorporation of PCL in itself thus seems to have a positive effect on the mechanical properties of film systems. However, higher values of these properties were obtained here (plantain flour/PCL blends processed by Rex) than in a previous study conducted by our research group using sagu flour/PCL blends processed by blending (Gutiérrez & Alvarez, 2017a).

The films that contained the catalyst (TPPF/PCL(80,000) + CAT) also showed improved mechanical properties compared to the films that did not (TPPF/PCL(80,000)) ($p \leq 0.05$) (Table 2). This fits well with the proposed cross-linking of the catalyst-containing blends. Similar behavior was observed by Gutiérrez & González (2017) for films derived from plantain flour cross-linked with *aloe vera* gel obtained by casting.

Finally, the highest toughness value was obtained for the TPPF/PCL (80,000) + CAT film. According to Gutiérrez & Alvarez (2017a) this could be very useful, as these films could absorb more energy thus

Table 2
Parameters of the uniaxial tensile strength tests: Young's modulus (E), maximum stress (σ_m), strain at break (ε_b) and toughness (T).

Material	E (MPa)	σ_m (MPa)	ε_b (%)	T ($\times 10^3$) (J/m^3)
TPPF	0.78 ± 0.06^a	1.1 ± 0.1^a	4 ± 1^a	3 ± 1^a
TPPF/PCL(10,000)	N.d.	N.d.	N.d.	N.d.
TPPF/PCL(10,000) + CAT	N.d.	N.d.	N.d.	N.d.
TPPF/PCL(80,000)	1.35 ± 0.04^b	2.1 ± 0.9^b	2.9 ± 0.6^a	4 ± 2^a
TPPF/PCL(80,000) + CAT	1.38 ± 0.02^b	3.4 ± 0.1^c	5.4 ± 0.3^b	12 ± 1^b

Equal letters in the same column indicate no statistically significant difference ($p \leq 0.05$).
Film systems: plantain flour (TPPF), plantain flour + PCL (M_w = 10,000 g/mol) (TPPF/PCL(10,000)), plantain flour + PCL (M_w = 10,000 g/mol) + catalyst (TPPF/PCL (10,000) + CAT), plantain flour + PCL (M_w = 80,000 g/mol) (TPPF/PCL(80,000)) and plantain flour + PCL (M_w = 80,000 g/mol) + catalyst (TPPF/PCL(80,000) + CAT).
Not determined: N.d.

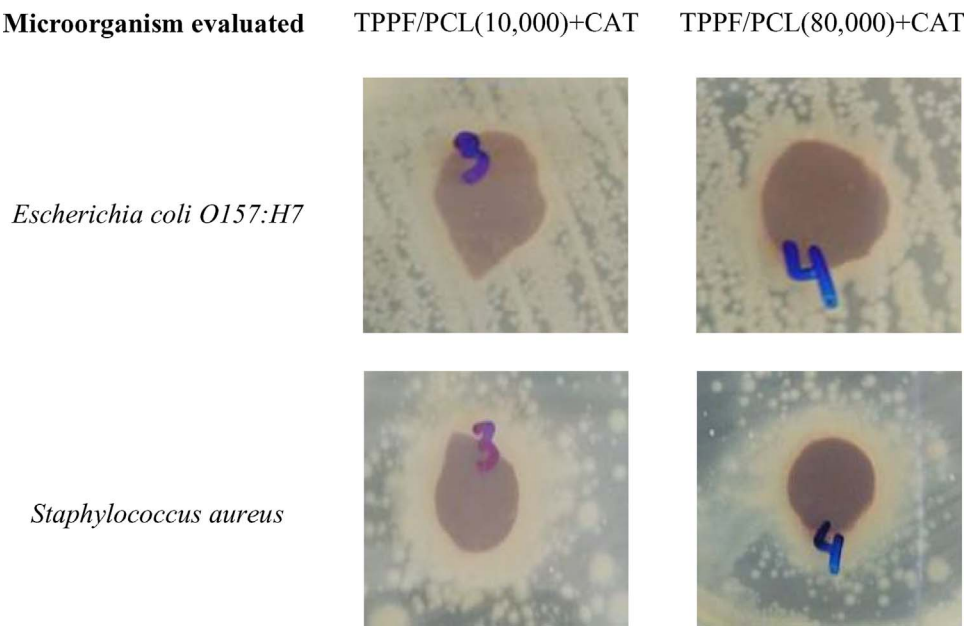

Fig. 7. Antimicrobial activity of the films studied: plantain flour + PCL (M_w = 10,000 g/mol) + catalyst (TPPF/PCL(10,000) + CAT) and plantain flour + PCL (M_w = 80,000 g/mol) + catalyst (TPPF/PCL (80,000) + CAT).

minimizing damage caused by knocks to foods during transport and storage. Nevertheless, all the toughness values obtained here are at least twice as low as those reported for films made from corn starch/PS blends using $Zn(Oct)_2$ under REx conditions (Gutiérrez & Alvarez, 2017b).

3.8. Antimicrobial activity

The antimicrobial activity of all the film systems was evaluated in order to establish whether they had potential as active packaging materials. As expected, the films prepared from plantain flour/PCL blends (TPPF/PCL(10,000) and TPPF/PCL(80,000)) showed no antimicrobial activity. In contrast, the films containing $Zr(Oct)_4$ (TPPF/PCL(80,000) + CAT and TPPF/PCL(10,000) + CAT) inhibited the growth of the two pathogenic microorganisms evaluated (*Escherichia coli O157:H7* and *Staphylococcus aureus*) (see Fig. 7), which is promising for the development of eco-friendly and active materials by REx. The dual effect of $Zr(Oct)_4$ (as a catalyst and an antimicrobial agent) is particularly interesting. This means that after generating cross-linking reactions between the polymers it remains within the polymer structure where it acts as an antimicrobial additive, making it an attractive alternative in the development of active food packaging. It is worth noting that the antimicrobial effect exhibited by $Zr(Oct)_4$ was effective against both the Gram-negative and the Gram-positive microorganisms evaluated indicating a broad antimicrobial spectrum. Both films containing the catalyst (TPPF/PCL(10,000) + CAT and TPPF/PCL(80,000) + CAT) showed the same degree of antimicrobial activity, with the susceptibility of the two microorganisms classified as "sensitive" according to the criteria used by Ponce et al. (2003). Conflicting results, however, were obtained by our research group using very low amount of Zn $(Oct)_2$ (approx. 1.90%) in starch/PS blends under REx conditions (Gutiérrez & Alvarez, 2017b). This could be due to three factors: (1) the catalyst content used in this study was 1.73 times greater (approx. 3.3%) than that employed in the study previously carried out using Zn $(Oct)_2$ (Gutiérrez & Alvarez, 2017b), (2) the concentration of the cation of the catalyst used here ($Zr(Oct)_4$) was at least twice that of the Zn $(Oct)_2$. It is well known that the anti-microbial effect depends on the concentration and type of cation of the organic salts typically used as antimicrobials, since this affects the oxidation-reduction potential for microbiological development (Jay, 1995), and (3) The matrices obtained in this study permitted a greater mobility of the catalyst within the polymer structure, thereby enabling its migration into the environment where it could act against the microorganisms. As regards this last point, it is worth remembering that the molecular spacing of the polymer chains was greater in the catalyst-containing films than in the films without the catalyst (see Section 3.5). This could explain the lower steric hindrance which permitted the catalyst to migrate towards the medium.

4. Conclusions

Films made from plantain flour/poly(ε-caprolactone) (PCL) blends were obtained under reactive extrusion (REx) conditions using zirconium octanoate ($Zr(Oct)_4$) as a catalyst. Films containing the catalyst showed cross-linking between the plantain flour and the PCL. The catalyst-containing films also showed antimicrobial activity against both the Gram-positive and Gram-negative pathogenic microorganisms studied (*E. coli O157:H7* and *S. aureus*) with both microorganisms being "sensitive" to their presence. This demonstrates that active eco-friendly films with improved properties can be obtained under REx conditions. The addition of PCL to the plantain flour gave films with improved properties compared to the films without this polymer. The use of high molecular weight (M_w) PCL in the blends reduced water sensitivity, whilst improving the thermal resistance and mechanical properties of the film systems.

Conflicts of interest

The authors declare no conflict of interest.

Acknowledgements

The authors would like to thank the Consejo Nacional de Investigaciones Científicas y Técnicas (CONICET) (Postdoctoral fellowship internal PDTS-Resolution 2417), Universidad Nacional de Mar del Plata (UNMdP) for financial support, and Dr. Mirian Carmona-Rodríguez.

References

Batista Reis, L. C., Oliveira de Souza, C., Alves da Silva, J. B., Martins, A. C., Larroza Nunes, I., & Druzian, J. I. (2015). Active biocomposites of cassava starch: The effect of yerba mate extract and mango pulp as antioxidant additives on the properties and the stability of a packaged product. *Food and Bioproducts Processing, 94*, 382–391. http://dx.doi.org/10.1016/j.fbp.2014.05.004.

Berruezo, M., Ludueña, L. N., Rodriguez, E., & Alvarez, V. A. (2014). Preparation and characterization of polystyrene/starch blends for packaging applications. *Journal of Plastic Film & Sheeting, 30*(2), 141–161. http://dx.doi.org/10.1177/8756087913504581.

Bertuzzi, M. A., Castro Vidaurre, E. F., Armada, M., & Gottifredi, J. C. (2007). Water vapor permeability of edible starch based films. *Journal of Food Engineering, 80*(3), 972–978. http://dx.doi.org/10.1016/j.jfoodeng.2006.07.016.

Biliaderis, C. G., Lazaridou, A., & Arvanitoyannis, I. (1999). Glass transition and physical properties of polyol-plasticised pullulan-starch blends at low moisture. *Carbohydrate Polymers, 40*(1), 29–47. http://dx.doi.org/10.1016/s0144-8617(99)00026-0.

Cheung, H.-Y., Lau, K.-T., Lu, T.-P., & Hui, D. (2007). A critical review on polymer-based bio-engineered materials for scaffold development. *Composites Part B: Engineering, 38*(3), 291–300. http://dx.doi.org/10.1016/j.compositesb.2006.06.014.

FDA (2016). *Indirect additives used in food contact substances.* Retrieved from https://www.accessdata.fda.gov/scripts/fdcc/index.cfm?set=IndirectAdditives&id=STANNOUSETHYLHEXANOATE.

García-Tejeda, Y. V., López-González, C., Pérez-Orozco, J. P., Rendón-Villalobos, R., Jiménez-Pérez, A., Flores-Huicochea, E., ... Bastida, C. A. (2013). Physicochemical and mechanical properties of extruded laminates from native and oxidized banana starch during storage. *LWT – Food Science and Technology, 54*(2), 447–455. http://dx.doi.org/10.1016/j.lwt.2013.05.041.

Gutiérrez, T. J., & Álvarez, K. (2016). Physico-chemical properties and in vitro digestibility of edible films made from plantain flour with added Aloe vera gel. *Journal of Functional Foods, 26*, 750–762. http://dx.doi.org/10.1016/j.jff.2016.08.054.

Gutiérrez, T. J., & Alvarez, V. A. (2017a). Films made by blending Poly(ε-caprolactone) with starch and flour from sagu rhizome grown at the venezuelan amazons. *Journal of Polymers and the Environment, 25*(3), 701–716. http://dx.doi.org/10.1007/s10924-016-0861-9.

Gutiérrez, T. J., & Alvarez, V. A. (2017b). Properties of native and oxidized corn starch/polystyrene blends under conditions of reactive extrusion using zinc octanoate as a catalyst. *Reactive and Functional Polymers, 112*, 33–44. http://dx.doi.org/10.1016/j.reactfunctpolym.2017.01.002.

Gutiérrez, T. J., & Alvarez, V. A. (2017c). Cellulosic materials as natural fillers in starch-containing matrix-based films: A review. *Polymer Bulletin, 74*(6), 2401–2430. http://dx.doi.org/10.1007/s00289-016-1814-0.

Gutiérrez, T. J., & González, G. (2017). Effect of cross-linking with Aloe vera gel on surface and physicochemical properties of edible films made from plantain flour. *Food Biophysics, 12*(1), 11–22. http://dx.doi.org/10.1007/s11483-016-9458-z.

Gutiérrez, T. J., Guarás, M. P., & Alvarez, V. A. (2017). Reactive extrusion for the production of starch-based biopackaging. In M. A. Masuelli (Ed.). *Biopackaging*Miami: CRC Press, Taylor & Francis Group. Retrieved from https://www.crcpress.com/Biopackaging/Masuelli/p/book/9781498749688.

Gutiérrez, T. J. (2017). Effects of exposure to pulsed light on molecular aspects of edible films made from cassava and taro starch. *Innovative Food Science & Emerging Technologies, 41*, 387–396. http://dx.doi.org/10.1016/j.ifset.2017.04.014.

Gutiérrez, T. J., Guzmán, R., Medina Jaramillo, C., & Famá, L. (2016). Effect of beet flour on films made from biological macromolecules: Native and modified plantain flour. *International Journal of Biological Macromolecules, 82*, 395–403. http://dx.doi.org/10.1016/j.ijbiomac.2015.10.020.

Gutiérrez, T. J., Morales, N. J., Pérez, E., Tapia, M. S., & Famá, L. (2015). Physico-chemical properties of edible films derived from native and phosphated cush–cush yam and cassava starches. *Food Packaging and Shelf Life, 3*, 1–8. http://dx.doi.org/10.1016/j.fpsl.2014.09.002.

Gutiérrez, T. J., Suniaga, J., Monsalve, A., & García, N. L. (2016). Influence of beet flour on the relationship surface-properties of edible and intelligent films made from native and modified plantain flour. *Food Hydrocolloids, 54*, 234–244. http://dx.doi.org/10.1016/j.foodhyd.2015.10.012.

Gutiérrez, T. J., Tapia, M. S., Pérez, E., & Famá, L. (2015). Edible films based on native and phosphated 80:20 waxy: Normal corn starch. *Starch/Staerke, 67*(1–2), 90–97. http://dx.doi.org/10.1002/star.201400164.

Hamann, D. D., Zhang, J., Daubert, C. R., Foegeding, E. A., & Diehl, K. C. (2006). Analysis of compression, tension and torsion for testing food gel fracture properties. *Journal of Texture Studies, 37*(6), 620–639. http://dx.doi.org/10.1111/j.1745-4603.2006.00074.x.

Hermans, P. H., & Weidinger, A. (1961). On the determination of the crystalline fraction of polyethylenes from X-ray diffraction. *Macromolecular Chemistry and Physics, 44*(1), 24–36. http://dx.doi.org/10.1002/macp.1961.020440103.

ISO 527-2 (2012). *Determination of tensile properties of plastics.* Retrieved from https://www.iso.org/obp/ui/#iso:std:56046:en.

Jay, J. M. (1995). Intrinsic and extrinsic parameters of foods that affect microbial growth. In J. M. Jay (Ed.). *Modern Food Microbiology* (pp. 38–66). (5th ed.). Boston, MA: Springer US. http://dx.doi.org/10.1007/978-1-4615-7476-7_3.

Kowalski, A., Duda, A., & Penczek, S. (1998). Kinetics and mechanism of cyclic esters polymerization initiated with tin(II) octoate, 1. Polymerization of ε-caprolactone. *Macromolecular Rapid Communications, 19*(11), 567–572. http://dx.doi.org/10.1002/(SICI)1521-3927(19981101)19:11<567::AID-MARC567>3.0.CO;2-T.

Labet, M., & Thielemans, W. (2009). Synthesis of polycaprolactone: A review. *Chemical Society Reviews, 38*(12), 3484–3504. http://dx.doi.org/10.1039/b820162p.

Loesecke, H. V. (1950). *Bananas.* New York: Interscience189.

Mali, S., Grossmann, M. V. E., Garcia, M. A., Martino, M. N., & Zaritzky, N. E. (2002). Microstructural characterization of yam starch films. *Carbohydrate Polymers, 50*(4), 379–386. http://dx.doi.org/10.1016/s0144-8617(02)00058-9.

Mathew, S., Brahmakumar, M., & Abraham, T. E. (2006). Microstructural imaging and characterization of the mechanical, chemical, thermal, and swelling properties of starch-chitosan blend films. *Biopolymers, 82*(2), 176–187. http://dx.doi.org/10.1002/bip.20480.

Merino, D., Ludueña, L. N., & Alvarez, V. A. (2017). Dissimilar tendencies of innovative green clay organo-modifier on the final properties of poly(ε-caprolactone) based nanocomposites. *Journal of Polymers and the Environment,* 1–12. http://dx.doi.org/10.1007/s10924-017-0994-5.

Mitrus, M. (2005). Glass transition temperature of thermoplastic starches. *International Agrophysics, 19*(3), 237–241. Retrieved from http://www.old.international-agrophysics.org/artykuly/international_agrophysics/IntAgr_2005_19_3_237.pdf.

Ninago, M. D., López, O. V., Lencina, M. M. S., García, M. A., Andreucetti, N. A., Ciolino, A. E., & Villar, M. A. (2015). Enhancement of thermoplastic starch final properties by blending with poly(ε-caprolactone). *Carbohydrate Polymers, 134*, 205–212. http://dx.doi.org/10.1016/j.carbpol.2015.08.007.

Ortega-Toro, R., Contreras, J., Talens, P., & Chiralt, A. (2015). Physical and structural properties and thermal behaviour of starch-poly(ε-caprolactone) blend films for food packaging. *Food Packaging and Shelf Life, 5*, 10–20. http://dx.doi.org/10.1016/j.fpsl.2015.04.001.

Pacheco, E. (2001). Evaluación nutricional de sopas deshidratadas a base de harina de plátano verde. Digestibilidad in vitro de almidón. *Acta Científica Venezolana, 52*(4), 278–282. Retrieved from http://acta.ivic.gob.ve/52-4/articulo6.pdf.

Pelissari, F. M., Andrade-Mahecha, M. M., do Amaral Sobral, P. J., & Menegalli, F. C. (2013). Comparative study on the properties of flour and starch films of plantain bananas (Musa paradisiaca). *Food Hydrocolloids, 30*(2), 681–690. http://dx.doi.org/10.1016/j.foodhyd.2012.08.007.

Penczek, S., Duda, A., Kowalski, A., Libiszowski, J., Majerska, K., & Biela, T. (2000). On the mechanism of polymerization of cyclic esters induced by tin(II) octoate. *Macromolecular Symposia, 157*(1), 61–70. http://dx.doi.org/10.1002/1521-3900(200007)157:1<61::AID-MASY61>3.0.CO;2-6.

Pereira, V. A., de Arruda, I. N. Q., & Stefani, R. (2015). Active chitosan/PVA films with anthocyanins from Brassica oleraceae (red cabbage) as time-temperature indicators for application in intelligent food packaging. *Food Hydrocolloids, 43*, 180–188. http://dx.doi.org/10.1016/j.foodhyd.2014.05.014.

Ponce, A. G., Fritz, R., del Valle, C., & Roura, S. I. (2003). Antimicrobial activity of essential oils on the native microflora of organic Swiss chard. *LWT – Food Science and Technology, 36*(7), 679–684. http://dx.doi.org/10.1016/S0023-6438(03)00088-4.

Raquez, J.-M., Narayan, R., & Dubois, P. (2008). Recent advances in reactive extrusion processing of biodegradable polymer-based compositions. *Macromolecular Materials and Engineering, 293*(6), 447–470. http://dx.doi.org/10.1002/mame.200700395.

Romero-Bastida, C. A., Bello-Pérez, L. A., García, M. A., Martino, M. N., Solorza-Feria, J., & Zaritzky, N. E. (2005). Physicochemical and microstructural characterization of films prepared by thermal and cold gelatinization from non-conventional sources of starches. *Carbohydrate Polymers, 60*(2), 235–244. http://dx.doi.org/10.1016/j.carbpol.2005.01.004.

Sanyang, M. L., Sapuan, S. M., Jawaid, M., Ishak, M. R., & Sahari, J. (2015). Effect of plasticizer type and concentration on tensile, thermal and barrier properties of biodegradable films based on sugar palm (Arenga pinnata) starch. *Polymers, 7*(6), 1106–1124. http://dx.doi.org/10.3390/polym7061106.

Shi, R., Zhang, Z., Liu, Q., Han, Y., Zhang, L., Chen, D., & Tian, W. (2007). Characterization of citric acid/glycerol co-plasticized thermoplastic starch prepared by melt blending. *Carbohydrate Polymers, 69*(4), 748–755. http://dx.doi.org/10.1016/j.carbpol.2007.02.010.

Tsuji, H., & Ishizaka, T. (2001). Porous biodegradable polyesters, 3. preparation of porous poly(ε-caprolactone) films from blends by selective enzymatic removal of poly(L-lactide). *Macromolecular Bioscience, 1*(2), 59–65. http://dx.doi.org/10.1002/1616-5195(20010301)1:2<59::AID-MABI59>3.0.CO;2-6.

Yu, L., Dean, K., & Li, L. (2006). Polymer blends and composites from renewable resources. *Progress in Polymer Science, 31*(6), 576–602. http://dx.doi.org/10.1016/j.progpolymsci.2006.03.002.